Configurational Statistics of Acyl Chains in Polyunsaturated Lipid Bilayers from ^2H NMR

Amir Salmon, Steven W. Dodd, Gerald D. Williams, James M. Beach, and Michael F. Brown*†

Contribution from the Department of Chemistry and Biophysics Program, University of Virginia, Charlottesville, Virginia 22901. *Received July 15, 1986*

Abstract: To gain a better understanding of the biological roles of polyunsaturated phospholipids, deuterium (^2H) NMR studies have been conducted of 1-perdeuteriopalmitoyl-2-docosahexaenoyl-*sn*-glycero-3-phosphocholine, an asymmetric or mixed-chain saturated–polyunsaturated phospholipid, in the liquid crystalline (L_α) phase. The palmitoyl (16:0) chain at the glycerol *sn*-1 position was labeled with ^2H by perdeuteration, whereas the polyunsaturated, docosahexaenoyl (22:6ω3) chain at the *sn*-2 position was unlabeled, i.e., protiated. The ^2H NMR results were compared to studies of 1,2-diperdeuteriopalmitoyl-*sn*-glycero-3-phosphocholine, in which both the *sn*-1 and *sn*-2 palmitoyl chains were perdeuterated, as well as 1-palmitoyl-2-perdeuteriopalmitoyl-*sn*-glycero-3-phosphocholine, in which only the *sn*-2 chain was perdeuterated. Multilamellar phospholipid dispersions containing 50 wt % H_2O were employed, and ^2H NMR spectra were obtained using quadrupolar echo methods at a magnetic field strength of 8.5 T. The experimental ^2H NMR spectra were numerically deconvoluted (de-Paked) to yield subspectra corresponding to the parallel bilayer orientation with respect to the main applied magnetic field. The increased resolution of the de-Paked subspectra enabled profiles of the segmental order parameters of the individual C–^2H bonds, denoted by $|S_{CD}(i)|$, to be derived as a function of chain position. Significant differences in the ^2H NMR spectra and derived $|S_{CD}(i)|$ profiles of the per-^2H-16:0 chains of the polyunsaturated and saturated bilayers were found. Based on simplified statistical mechanical theories, the differences can be interpreted in terms of an increase in the configurational freedom of the palmitoyl chains in the polyunsaturated bilayer, relative to bilayers of phosphatidylcholines with two identical saturated chains. The increased configurational freedom may correspond to an increase in the equilibrium area per chain in the case of the polyunsaturated bilayer. Possible further interpretations of the results in terms of the thickness of the hydrocarbon region and the presence or lack of interdigitation of the polyunsaturated and saturated acyl chains are also briefly discussed. We conclude that the configurational properties of the acyl chains of polyunsaturated bilayers are significantly different from those of saturated phospholipid bilayers.

1. Introduction

Deuterium nuclear magnetic resonance (^2H NMR) can provide structural and dynamic knowledge at the atomic level for lipid bilayers and biomembranes, in the liquid-crystalline (L_α) phase.[1-4] Such information is not currently obtainable using other techniques such as X-ray diffraction.[5,6] Lately, polyunsaturated lipids[7] have attracted considerable attention in view of their roles as precursors to prostaglandins,[8-10] thromboxanes,[9] and leukotrienes,[11] because of their presence in visual photoreceptor membranes,[12] and owing to evidence linking them with cardiovascular disease,[13] visual disorders,[14] cancer,[15] and aging.[15,16] In spite of their widespread occurrence and biological importance, however, relatively little is known of the structural and dynamic properties of polyunsaturated phospholipids in membranes. As a step toward achieving a better understanding of their biological roles, we have applied ^2H NMR methods to the problems of defining the average structural properties of polyunsaturated phospholipids in the liquid-crystalline phase, and delineating any similarities or differences with respect to the corresponding properties of bilayers of saturated phospholipids. In this paper, we describe ^2H NMR studies of 1-palmitoyl-2-docosahexaenoyl-*sn*-glycero-3-phosphocholine, an asymmetric or mixed-chain saturated-polyunsaturated phospholipid, whose structure is indicated below:

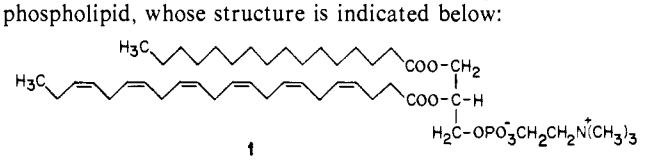

1

Docosahexaenoic acid (22:6ω3) is the major fatty acid constituent of the retinal rod outer segment disk membrane phospholipids,[12] and is known to be an inhibitor of prostaglandin biosynthesis.[10] We report the characteristic ^2H NMR signatures of the polyunsaturated phospholipid **1** in the L_α phase, in which the palmitoyl (16:0) chain is perdeuterated, and show how the differences relative to saturated phospholipid bilayers[1-3,17] can be interpreted in terms of simplified models for their acyl chain configurational statistics.

† Alfred P. Sloan Research Fellow.

2. Experimental Section

We refer[18] to the phospholipid **1** with a perdeuterated, palmitic acid (16:0) chain at the glycerol *sn*-1 position and a protiated, docosahexae-

(1) Seelig, J. *Q. Rev. Biophys.* **1977**, *10*, 353-418.
(2) Seelig, J.; Seelig, A. *Q. Rev. Biophys.* **1980**, *13*, 19-61.
(3) Davis, J. H. *Biochim. Biophys. Acta* **1983**, *737*, 117-171.
(4) Brown, M. F.; Williams, G. D. *J. Biochem. Biophys. Meth.* **1985**, *11*, 71-81.
(5) Luzzati, V. In *Biological Membranes Physical Fact and Function*; Chapman, D., Ed.; Academic: New York, 1968; pp 71-123.
(6) Blaurock, A. E. *Biochim. Biophys. Acta* **1983**, *650*, 167-207.
(7) Kunau, W.-H. *Angew. Chem., Int. Ed. Engl.* **1976**, *15*, 61-122.
(8) Samuelsson, B.; Granström, E.; Green, K.; Hamberg, M.; Hammarström, S. *Annu. Rev. Biochem.* **1975**, *44*, 669-695.
(9) Samuelsson, B.; Goldyne, M.; Granström, E.; Hamberg, M.; Hammarström, S.; Malmsten, C. *Annu. Rev. Biochem.* **1978**, *47*, 997-1029.
(10) Corey, E. J.; Shih, C.; Cashman, J. R. *Proc. Natl. Acad. Sci. U.S.A.* **1983**, *80*, 3581-3584.
(11) Hammarström, S. *Annu. Rev. Biochem.* **1983**, *52*, 355-377.
(12) Stone, W. L.; Farnsworth, C. C.; Dratz, E. A. *Exp. Eye Res.* **1979**, *28*, 387-397.
(13) (a) Dyerberg, J.; Bang, H. O. *Lancet i* **1978**, 152. (b) Dyerberg, J.; Bang, H. O.; Stoffersen, E.; Moncada, S.; Vane, J. R. *Lancet ii* **1978**, 117-119. (c) Glomset, J. A. *New. Eng. J. Med.* **1985**, *312*, 1253-1254.
(14) (a) Wheeler, T. G.; Benolken, R. M.; Anderson, R. E. *Science* **1975**, *188*, 1312-1314. (b) Katz, M. L.; Stone, W. L.; Dratz, E. A. *Invest. Ophthalmol. Visual Sci.* **1978**, *17*, 1049-1058. (c) Katz, M. L.; Parker, K. R.; Handelman, G. J.; Bramel, T. J.; Dratz, E. A. *Exp. Eye Res.* **1982**, *34*, 339-369. (d) Neuringer, M.; Connor, W. E.; Van Petten, C.; Barstad, L. *J. Clin. Invest.* **1984**, *73*, 272-276. (e) Neuringer, M.; Conner, W. E.; Lin, D. S.; Barstad, L.; Luck, S. *Proc. Natl. Acad. Sci. U.S.A.* **1986**, *83*, 4021-4025.
(15) Ames, B. N. *Science* **1983**, *221*, 1256-1264.
(16) Harman, D. *Proc. Natl. Acad. Sci. U.S.A.* **1981**, *78*, 7124-7128.
(17) Schindler, H.; Seelig, J. *Biochemistry* **1975**, *14*, 2283-2287.
(18) Abbreviations used: (per-^2H-16:0)(22:6)PC, 1-perdeuteriopalmitoyl-2-docosahexaenoyl-*sn*-glycero-3-phosphocholine; di(per-^2H-16:0)PC, 1,2-diperdeuteriopalmitoyl-*sn*-glycero-3-phosphocholine; (16:0)(per-^2H-16:0)PC, 1-palmitoyl-2-perdeuteriopalmitoyl-*sn*-glycero-3-phosphocholine; BHT, butylated hydroxytoluene; EDTA, ethylenediaminetetracetic acid; ODF, order-director fluctuations.

0002-7863/87/1509-2600$01.50/0

noic acid (22:6) chain at the *sn*-2 position as (per-^{2}H-16:0)(22:6)PC. The corresponding saturated phospholipid with two perdeuterated acyl chains, viz., 1,2-diperdeuteriopalmitoyl-*sn*-glycero-3-phosphocholine, is denoted by di(per-^{2}H-16:0)PC. Finally, 1-palmitoyl-2-perdeuteriopalmitoyl-*sn*-glycero-3-phosphocholine, i.e., in which only the *sn*-2 palmitoyl chain is perdeuterated, is indicated as (16:0)(per-^{2}H-16:0)PC. The above phospholipids were synthesized and characterized as described,[19,20] except that all procedures involving unsaturated compounds were conducted under an inert argon atmosphere, using solvents containing butylated hydroxytoluene (BHT). The final molar ratio of BHT to (per-^{2}H-16:0)(22:6)PC was ~1/500. All *cis*-4,7,10,13,16,19-docosahexaenoic acid was obtained from Nu Chek Prep, Inc. (Elysian, MN). The isomeric purity of the (per-^{2}H-16:0)(22:6)PC product was determined by treating it with snake venom phospholipase A_2 from *Crotalus adamanteus* (E.C. 3.1.1.4) (Sigma, MO), followed by transesterification of the *sn*-2 hydrolyzed fatty acids with BCl_3/MeOH (Supelco, PA), and their identification by use of gas–liquid chromatography. No acyl chain migration (<2%) was detected. For the case of (16:0)(per-^{2}H-16:0)PC, the protiated and perdeuterated palmitic acid methyl esters were identified by capillary gas–liquid chromatography using a 0.25-mm i.d. × 30-m column (0.25 μ thickness DB-1 bonded phase; Scientific Products, IL); little or no acyl chain migration was found. Samples of phospholipids containing 200–250 mg were prepared for ^{2}H NMR spectroscopy by lyophilization from cyclohexane/$CHCl_3$, ~20/1 (v/v), followed by addition of an equal weight of 0.067 M sodium phosphate buffer prepared from ^{2}H-depleted ^1H_2O (Aldrich, WI), containing 10^{-4} M EDTA and 0.01 wt % NaN_3 at pH 7.0. The 50 wt % phospholipid dispersions were briefly vortexed (<1 min) above their main thermal-phase transition temperatures in 10-mm Pyrex culture tubes and centrifuged; Teflon plugs were inserted. The tubes were then cut off and their edges sealed with high-melting (90 °C) wax (Petrolite, OK). When not in use, the phospholipid dispersions were stored at −20 or −85 °C. Thin layer chromatography of the samples before and after ^{2}H NMR spectroscopy with silica gel G plates (250 μ thickness; Analab, DE) eluted with $CHCl_3$/MeOH/H_2O (65/35/5) gave single spots after charring with 40% H_2SO_4 in EtOH.

^{2}H NMR studies were performed at a magnetic field strength of 8.481 T (^{2}H frequency of 55.43 MHz) as described.[20] The quadrupolar echo method[21,22] was employed with a pulse spacing of 60 μs; little change in spectral shape was observed over the range of pulse intervals 40 to 200 μs. Care was taken to initiate the Fourier transformation at the maximum of the quadrupolar echo.[3] The experimental ^{2}H NMR spectra were transferred to a CDC Cyber 180/855 main-frame computer, and numerically deconvoluted to obtain the subspectra corresponding to the θ = 0° orientation of the bilayer normal relative to the main magnetic field, using the de-Pakeing algorithm of Bloom et al.[23,24] Control studies of (perdeuterated) potassium palmitate-d_{31} in the L_α phase[25] showed that the integrated areas of the de-Paked ^{2}H NMR spectral components were proportional to the number of deuterons, to within experimental error (not shown). The C–^{2}H bond segmental order parameters were evaluated from the sharp edges of the experimental, powder-type ^{2}H NMR spectra, due to the θ = 90° orientation, as well as from the de-Paked subspectra arising from the θ = 0° orientation, using the expression[1]

$$\Delta\nu_Q(i) = {}^3/_2(e^2qQ/h)P_2(\cos\theta)|S_{CD}(i)| \quad (1)$$

In the above, $\Delta\nu_Q(i)$ denotes the residual quadrupolar splitting of the ith deuterated segment, and P_2 is the second Legendre polynomial. The C–^{2}H bond segmental order parameter $S_{CD}(i)$ is a quantitative and unambiguous measure of the extent of the orientational disorder at a particular ^{2}H-labeled segment. It is defined as[1-3]

$$S_{CD}(i) \equiv \langle P_2(\cos\beta_i(t))\rangle \equiv {}^1/_2\langle 3\cos^2\beta_i(t) - 1\rangle \quad (2)$$

Here the brackets indicate an average over all C-^{2}H bond orientations sampled on a time scale less than the inverse of the static quadrupolar interaction (10^{-6} s); and $\beta_i(t)$ is the time-dependent angle between the C–^{2}H bond direction and the average bilayer normal. A value of (e^2qQ/h) = 170 kHz was taken for the static quadrupolar coupling constant.[1]

3. Results

Different ^{2}H NMR Spectra Are Observed for Polyunsaturated and Saturated Phospholipid Bilayers. Figure 1a,b shows ^{2}H NMR spectra of aqueous dispersions of (per-^{2}H-16:0)(22:6)PC and di(per-^{2}H-16:0)PC, containing 50 wt % H_2O in the L_α phase at 323 K (50 °C), respectively. The experimental ^{2}H NMR spectra (lower) are seen in each case to consist of a series of overlapping powder patterns, i.e., Pake doublets, arising from the various inequivalent deuterated chain segments.[26] The sharp spectral features or edges correspond to the θ = 90° orientation of the bilayer normal relative to the main magnetic field direction, and the well-defined shoulders with less intensity represent the θ = 0° orientation.[1-3] The observed ^{2}H NMR spectral line shapes are indicative of a largely random bilayer distribution;[3] orientation effects due to the magnetic field[27,28] are not seen. Assuming that the quadrupolar splittings scale with the bilayer orientation as $P_2(\cos\theta)$, the experimental powder-type ^{2}H NMR spectra (lower) were deconvoluted, i.e., de-Paked,[23,24] to yield the subspectra (upper) corresponding to the θ = 0° orientation. The residual quadrupolar splittings of the de-Paked ^{2}H NMR spectra are twice those of the θ = 90° edges of the experimental spectra; cf. eq 1. The increased resolution is due to the fact that the deconvoluted subspectra are spread out to their fullest extent, and correspond to a single bilayer orientation.

For the limiting case of an all-trans chain rotating about its long axis, a quadrupolar splitting of 63.75 kHz would be expected for the sharp θ = 90° edges of the methylene powder patterns, assuming a value of 170 kHz for the static quadrupolar coupling constant.[1] The corresponding splitting for the terminal C^2H_3 groups would be 21.25 kHz; because of the C_{3v} symmetry, the electrostatic field gradient is projected onto the last carbon–carbon bond axis of the chain. The observed ^{2}H NMR spectra (Figure 1) of the two bilayers thus allow one to conclude immediately that in each case the chains are orientationally disordered relative to the bilayer normal, the symmetry axis for the motional averaging.[1] In the case of the (per-^{2}H-16:0)(22:6)PC bilayer, the observed quadrupolar splittings of the methylene groups fall into the range of 22.6 to 5.41 kHz for the θ = 90° spectral edges, with a terminal methyl splitting of 1.48 kHz. From studies of specifically deuterated phosphatidylcholines in the L_α phase,[1] it is known that the largest residual quadrupolar splittings correspond to those C^2H_2 segments closest to the aqueous interface, with a progressive decrease along the chains toward the terminal methyl groups. The time scale for motional averaging of the ^{2}H NMR spectra is defined by the reciprocal of the rigid-limit or static interaction strength [${}^3/_2(e^2qQ/h)$ = 255 kHz], so that fluctuations with angular correlation times of less than 10^{-6} s contribute to the residual quadrupolar splittings.

As can be seen in Figure 1, differences are indeed evident in the ^{2}H NMR spectra of the multilamellar dispersions of (per-^{2}H-16:0)(22:6)PC and di(per-^{2}H-16:0)PC in the L_α phase, at the same absolute temperature of 323 K. Qualitatively, the ^{2}H NMR spectra of the (per-^{2}H-16:0)(22:6)PC bilayer (Figure 1a) appear more reminiscent of a single-chain amphiphile in the L_α phase, such as potassium palmitate,[25] than of a phospholipid with two identical saturated acyl chains,[20,26] such as di(per-^{2}H-16:0)PC (Figure 1b). The resolution of distinct spectral features with separations ≤1–2 kHz in each case suggests that ultraslow motional processes[29-31] do not greatly influence the ^{2}H NMR spectral line shapes, or account for the observed differences. The powder-type ^{2}H NMR spectrum (Figure 1a, lower) of the dis-

(19) Mason, J. T.; Broccoli, A. V.; Huang, C. *Anal. Biochem.* **1981**, *113*, 96–101.
(20) Williams, G. D.; Beach, J. M.; Dodd, S. W.; Brown, M. F. *J. Am. Chem. Soc.* **1985**, *107*, 6868–6873.
(21) Davis, J. H.; Jeffrey, K. R.; Bloom, M.; Valic, M. I.; Higgs, T. P. *Chem. Phys. Lett.* **1976**, *42*, 390–394.
(22) Bloom, M.; Davis, J. H.; Valic, M. I. *Can. J. Phys.* **1980**, *58*, 1510–1517.
(23) Bloom, M.; Davis, J. H.; MacKay, A. L. *Chem. Phys. Lett.* **1981**, *80*, 198–202.
(24) Sternin, E.; Bloom, M.; MacKay, A. L. *J. Magn. Reson.* **1983**, *55*, 274–282.
(25) Davis, J. H.; Jeffrey, K. R. *Chem. Phys. Lipids* **1977**, *20*, 87–104.
(26) Davis, J. H. *Biophys. J.* **1979**, *27*, 339–358.
(27) Forrest, B. J.; Reeves, L. W. *Chem. Rev.* **1981**, *81*, 1–14.
(28) Seelig, J.; Borle, F.; Cross, T. A. *Biochim. Biophys. Acta* **1985**, *814*, 195–198.
(29) Campbell, R. F.; Meirovitch, E.; Freed, J. H. *J. Phys. Chem.* **1979**, *83*, 525–533.
(30) Burnell, E. E.; Cullis, P. R.; De Kruijff, B. *Biochim. Biophys. Acta* **1980**, *603*, 63–69.
(31) Brown, M. F.; Davis, J. H. *Chem. Phys. Lett.* **1981**, *79*, 431–435.

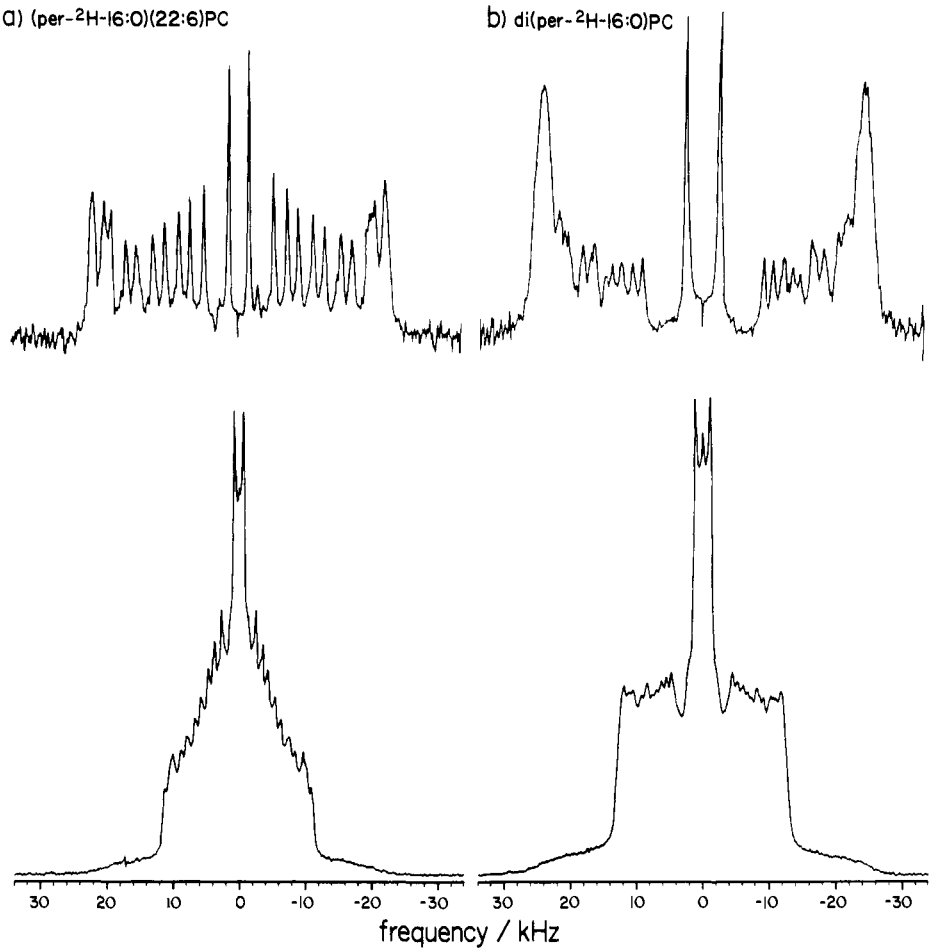

Figure 1. Comparison of ^2H NMR spectra of polyunsaturated and saturated phospholipid bilayers in the L_α phase. ^2H NMR spectra are shown of dispersions of (a) (per-^2H-16:0)(22:6)PC and (b) di(per-^2H-16:0)PC, containing 50 wt% H_2O at 323 K (50 °C). In each case, the experimental ^2H NMR spectrum of the randomly oriented, multilamellar dispersion is plotted on the same frequency axis immediately below the oriented subspectrum obtained by numerical deconvolution (de-Pakeing). Note the different vertical scales of the experimental and de-Paked ^2H NMR spectra.

persion of (per-^2H-16:0)(22:6)PC in the L_α phase, i.e., in which the palmitoyl chain at the glycerol *sn*-1 position is perdeuterated, appears roughly triangular in shape; the sharp component with the smallest quadupolar splitting arises from the chain terminal C^2H_3 groups. In the de-Paked ^2H NMR spectrum (Figure 1a, upper), eleven different quadrupolar splittings are clearly resolved, corresponding to the various C^2H_2 groups and terminal C^2H_3 group of the palmitoyl (16:0) chain at the glycerol *sn*-1 position. We have assumed that the resolved components with de-Paked quadrupolar splittings intermediate between the smallest and largest values ($\Delta\nu_Q$ = 10.8 to 39.4 kHz) arise from individual C^2H_2 groups of the acyl chains, rather than to inequivalence of their two deuterons, which is consistent with the relative areas of the spectral peaks.

By contrast, the powder-type ^2H NMR spectrum of di(per-^2H-16:0)PC in the L_α phase (Figure 1b, lower), i.e., with two perdeuterated palmitoyl chains, appears more rectangular in shape, with a sharp terminal C^2H_3 splitting. The approximately rectangular shape, with a sharp falloff of intensity to either side, is indicative of a plateau in the distribution of residual quadrupolar splittings and derived C–^2H bond segmental order parameters as a function of chain position.[3,26,32] The corresponding de-Paked ^2H NMR spectrum (Figure 1b, upper) differs from that of the (per-^2H-16:0)(22:6)PC bilayer (Figure 1a, upper) in that significantly more intensity is present in the components with largest quadrupolar splittings. The latter arise from the C^2H_2 groups toward the esterified terminus of the chain, which are comparable in their motional properties and give rise to the plateau in the order profile.[32] The other components with de-Paked quadrupolar splittings of $\Delta\nu_Q$ = 18.9 to 44.8 kHz arise from the various inequivalent C^2H_2 groups of the two acyl chains, for which the two deuterons give rise to the same splitting,[1-3,32] as well as the two inequivalent deuterons of the C_2 segment of the *sn*-2 acyl chain;[1,33,34] the smallest splitting is due to the chain terminal C^2H_3 groups. The observed differences in the ^2H NMR spectra of the (per-^2H-16:0)(22:6)PC bilayer and the di(per-^2H-16:0)PC bilayer, in the L_α phase, suggest that conformation-dependent properties of the palmitoyl chains vary in the two cases.

Order Profiles of Polyunsaturated and Saturated Bilayers. Figure 2 shows plots of the C-^2H bond segmental order parameters $|S_{CD}(i)|$, derived from the de-Paked ^2H NMR spectra shown in Figure 1, as a function of the chain segment index *i*. Significant differences are apparent in the order profiles of the palmitoyl chains of the (per-^2H-16:0)(22:6)PC bilayer and the di(per-^2H-16:0)PC bilayer, in the L_α phase, at the same absolute temperature of 323 K. The profile for the di(per-^2H-16:0)PC bilayer was assigned based on integrated intensities of the de-Paked ^2H NMR spectra and comparison to previous results for di(16:0)PC with specifically deuterated acyl chains.[32,33,35]. The order profiles derived from the de-Paked ^2H NMR spectra are in good agreement with earlier studies[36] of di(per-^2H-16:0)PC. Because of their different initial orientations with respect to the bilayer surface,[1,2,33] separate profiles are obtained for the *sn*-1 and *sn*-2 chains. These were assigned by comparison to results acquired for bilayers of (16:0)(per-^2H-16:0)PC, i.e., in which only the *sn*-2 acyl chain was perdeuterated (not shown); similar data have been reported by

(32) Seelig, A.; Seelig, J. *Biochemistry* **1974**, *13*, 4839–4845.
(33) Seelig, A.; Seelig, J. *Biochim. Biophys. Acta* **1975**, *406*, 1–5.
(34) Seelig, J.; Browning, J. L. *FEBS Lett.* **1978**, *92*, 41–44.
(35) Brown, M. F.; Seelig, J.; Häberlen, U. *J. Chem. Phys.* **1979**, *70*, 5045–5053.
(36) Pauls, K. P.; MacKay, A. L.; Bloom, M. *Biochemistry* **1983**, *22*, 6101–6109.

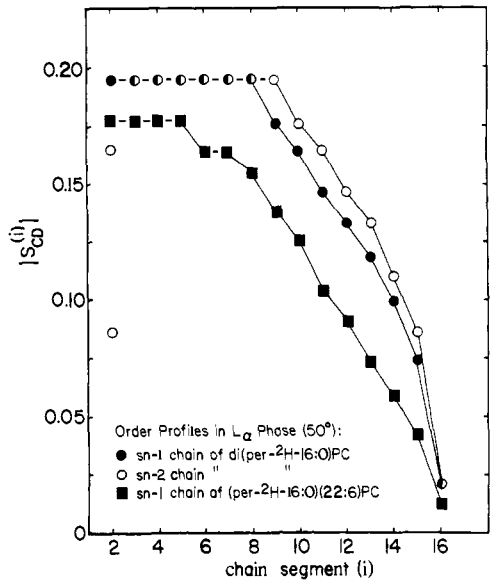

Figure 2. Comparison of C–^{2}H bond segmental order parameters of polyunsaturated and saturated phospholipid bilayers in the L_α phase. Absolute values of the orientational order parameters of the C–^{2}H bond segments $|S_{CD}(i)|$ are plotted as a function of the acyl chain index i, beginning with the C_2 segment adjacent to the ester carbonyl carbon. The data refer to the palmitoyl (16:0) chains of the (per-^{2}H-16:0)-(22:6)PC bilayer and the di(per-^{2}H-16:0)PC bilayer at 323 K (50 °C). The profiles were derived from the de-Paked ^{2}H NMR spectra shown in Figure 1: (●) *sn*-1 and (○) *sn*-2 chains of di(per-^{2}H-16:0)PC bilayer; (■) *sn*-1 chain of (per-^{2}H-16:0)(22:6)PC bilayer. Owing to the nonidentical initial orientations, different order parameters are obtained for the C_2 methylene segments of the two chains of the di(per-^{2}H-16:0)PC bilayer; in addition, the two deuterons of the C_2 segment of the *sn*-2 chain are inequivalent.[1,33,34] The points joined by dashed lines correspond to segments whose quadrupolar splittings were not resolved in the de-Paked ^{2}H NMR spectra. At the same absolute temperature, the *sn*-1 chain of the polyunsaturated bilayer is more disordered and the plateau in the order profile is shorter than for the disaturated bilayer.

Paddy et al.[37] The profile of the $|S_{CD}(i)|$ values of the palmitoyl chain at the *sn*-1 position of the (per-^{2}H-16:0)(22:6)PC bilayer (Figure 2) was assigned based on integrated areas and the assumption that the quadrupolar splittings decrease along the chain as seen for di(per-^{2}H-16:0)PC in the L_α phase. Figure 2 shows that the $|S_{CD}(i)|$ values of all the segments of the palmitoyl chain are less when esterified next to a 22:6 chain, at the *sn*-2 position of the (per-^{2}H-16:0)(22:6)PC bilayer, than is the case in bilayers of di(per-^{2}H-16:0)PC at the same absolute temperature. The length of the plateau representing those C^2H_2 groups nearest the aqueous interface is also less in the former case.

Order profiles obtained for the *sn*-1 chains of the (per-^{2}H-16:0)(22:6)PC bilayer and the di(per-^{2}H-16:0)PC bilayer are compared at different temperatures in the L_α phase in Figure 3. In each case, the segmental order parameters decrease with increasing temperature, consistent with previous results.[32] For the case of the (per-^{2}H-16:0)(22:6)PC bilayer, the main order–disorder phase transition occurs near $T_c \simeq 263$ K (−10 °C) (not shown); for the di(per-^{2}H-16:0)PC bilayer the phase transition temperature is $T_c = 310$ K (37 °C).[26] The absolute temperatures in Figure 3 have been chosen such that the order profiles of the two bilayers correspond to approximately the same reduced temperatures, defined[34] as $T_{red} \equiv (T - T_c)/T_c$. As can be seen in Figure 3, the length of the plateau in the $|S_{CD}(i)|$ profiles obtained for the *sn*-1 chain of the (per-^{2}H-16:0)(22:6)PC bilayer is roughly constant as a function of temperature, and is less than that of the *sn*-1 chain of the di(per-^{2}H-16:0)PC bilayer at each of the reduced temperatures investigated. Whereas the polyunsaturated bilayer is less ordered than the disaturated bilayer at the same absolute temperature (Figure 2), at equivalent reduced temperatures (Figure 3) the $|S_{CD}(i)|$ values are greater in the former case. These observations imply that the differences in the order profiles of the two bilayers reflect inherent dissimilarities in the configurational properties of the saturated acyl chains at the *sn*-1 position, and are not simply a consequence of the $\gtrsim$50 °C difference in their main order–disorder transition temperatures.

4. Discussion

The profiles of the segmental order parameters $S_{CD}(i)$ provide a quantitative measure of the orientational ordering of the acyl chains of phospholipids in the liquid-crystalline state with respect to the macroscopic bilayer normal. As experimental observables, the C–^{2}H bond segmental order parameters are equal to the time- or ensemble-averaged values of the second-rank spherical harmonics $Y_0^{(2)}(\beta_i;t)$, that is, the second Legendre polynomials $P_2(\cos \beta_i;t)$, where $\beta_i;t$ denotes the instantaneous angle between a C–^{2}H bond vector attached to the ith segment and the director axis.[4] For the case of lipid bilayers in the L_α phase (cf. Figure 2), the absolute magnitudes of the order parameters as a function of chain segment position are observed to fall between the values expected of an all-trans polymethylene chain rotating about its long axis [$S_{CD}(i) = -1/2$], and for complete orientational disorder as found in isotropic fluids [$S_{CD}(i) = 0$]. The hydrocarbon region of a lipid bilayer must thus exist in a state of intermediate order; the chains are substantially disordered and are liquid-like in their character,[4] yet residual order persists as expected of a solid.[1] It is the configurational properties of the acyl chains of lipid bilayers in the liquid-crystalline state that are of interest insofar as the averaged structural properties of the hydrocarbon region are concerned. From the experimental ^{2}H NMR order profiles, it can be concluded that the orientational ordering of the methylene segments is roughly constant over the first part of the chain; i.e., a plateau is observed followed by a progressive decrease in the segmental ordering toward the chain ends. The observation of a plateau in the distribution of the order parameters $|S_{CD}(i)|$ as a function of the acyl chain segment position suggests that the conformations responsible for the disordering occur with roughly equal probability over the initial part of the chains. Moreover, the present work has shown that the ^{2}H NMR spectra and derived order profiles are very sensitive to esterification of a saturated fatty acyl chain adjacent to a polyunsaturated chain in bilayers composed of asymmetric, mixed-chain saturated–polyunsaturated phospholipids. Compared to the di(per-^{2}H-16:0)PC bilayer at the same absolute temperature, the palmitoyl chain at the *sn*-1 position of the (per-^{2}H-16:0)(22:6)PC bilayer is more disordered, and the plateau in the order profile is significantly shorter. In order to further interpret the ^{2}H NMR data, one must introduce models for the acyl chain configurational statistics.

What is the molecular basis for the different order profiles observed for the polyunsaturated and saturated phospholipids in the L_α phase, and how can one further explain the results in terms of interaction strengths related to thermodynamic properties of lipid bilayers? Owing to their physical complexity, entirely general statistical models for lipid bilayers are not feasible at present.[38] Thus, in applying the formalisms of statistical mechanics to lipid bilayers, two broadly interrelated approaches have been taken.[38] First, simplification can be introduced at the level of the specific physical model considered, so that more or less exact calculations are possible; representative examples include the lattice theories of Nagle[39] and Dill and Flory.[40] Alternately, somewhat more complex, but more realistic physical models can be considered, and simplification introduced at the level of controlled mathematical approximations involving adjustable parameters whose physical significance may be reduced; examples of the latter include the mean-field theories of Marčelja[41] and Meraldi and Schlitter.[42,43] In our discussion, we will naturally tend to emphasize the latter semiempirical approach, which is most closely

(37) Paddy, M. R.; Dahlquist, F. W.; Dratz, E. A.; Deese, A. J. *Biochemistry* **1985**, *24*, 5988–5995.

(38) Nagle, J. F. *Annu. Rev. Phys. Chem.* **1980**, *31*, 157–195.
(39) Nagle, J. F. *J. Chem. Phys.* **1975**, *63*, 1255–1261.
(40) Dill, K. A.; Flory, P. J. *Proc. Natl. Acad. Sci. U.S.A.* **1980**, *77*, 3115–3119.
(41) Marčelja, S. *Biochim. Biophys. Acta* **1974**, *367*, 165–176.

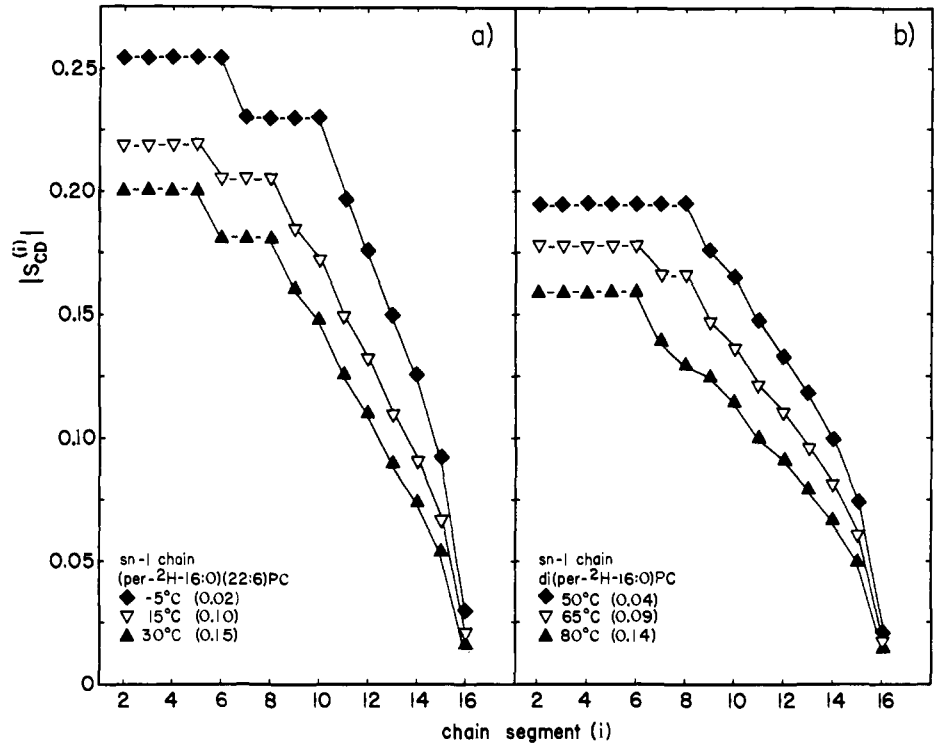

Figure 3. Order profiles of polyunsaturated and saturated phospholipid bilayers at different absolute and reduced temperatures (see text). In each case, the values of $|S_{CD}(i)|$ are plotted as a function of the chain position i. Data are shown for the *sn*-1 chains of (a) (per-^{2}H-16:0)(22:6)PC and (b) di(per-^{2}H-16:0)PC in the L_α phase. For the case of the (per-^{2}H-16:0)(22:6)PC bilayer, the symbols refer to absolute temperatures (reduced temperatures) of (♦) 268 K (0.02), (▽) 288 K (0.10), and (▲) 303 K (0.15). For the di(per-^{2}H-16:0)PC bilayer, the symbols indicate absolute temperatures (reduced temperatures) of (♦) 323 K (0.04), (▽) 338 K (0.09), and (▲) 353 K (0.14). Note that at approximately equivalent reduced temperatures, the *sn*-1 chains of the polyunsaturated bilayer are more ordered than those of the disaturated bilayer, whereas the opposite is true at the same absolute temperature.

rooted in the experimental ^{2}H NMR data obtained for lipid bilayers in the liquid-crystalline state.

Intermolecular Forces in Lipid Bilayers. We shall first discuss the factors which influence the molecular organization of phospholipids in membranes, before turning to a more detailed interpretation of the experimental ^{2}H NMR results. In discussing the physical properties of lipid bilayers, it is often valuable to make reference to studies of structurally less complex systems. Current knowledge of the averaged structures of simple fluids and solids is summarized by generalized van der Waals theory.[44,45] In this unified picture, emphasis is placed upon the different roles of relatively strong, short-ranged intermolecular repulsive forces and weaker, longer ranged attractive interactions in determining the averaged structure and dynamical properties of the system. The averaged intermolecular arrangements and motions of the molecules are dictated primarily by the local packing and steric effects produced by short-ranged, repulsive interactions, which are related to the sizes and shapes of the constituent molecules. The attractive forces, which include permanent and induced electric dipolar interactions and other interactions which vary weakly with distance, play a relatively minor role in determining the structure, and provide the cohesive energy necessary to fix the volume of the system to within relatively narrow limits at a given temperature and pressure. The longer-ranged, attractive interactions can be described in terms of a mean or molecular field approximation; that is, a spatially uniform background potential through which an individual molecule interacts with its neighbors. For the case of nematic and other liquid-crystalline mesophases, the relative importance of short- and long-ranged interactions in governing their averaged structure or ordering and phase transitions has been rather controversial in the past. As is the case for simple liquids, the generalized van der Waals theory for molecules interacting through angularly dependent potentials can be broken up into relatively strong, short-ranged steric repulsive interactions, and weaker long-ranged attractions. One school of thought has assumed that the nematic ordering arises primarily from the anisotropy of the longer-ranged dispersion forces; the intermolecular repulsive interactions are largely neglected.[46,47] By contrast, a second line of thinking has envisaged the averaged structure to be governed primarily by short-ranged, highly anisotropic repulsive forces, due to electronic overlap, as in the above van der Waals picture of liquids and solids. The longer-ranged, intermolecular attractive forces are assumed to mainly provide cohesion and to stabilize the system.[48-50] At present, agreement exists in that the short-ranged repulsive forces appear to play the major role in governing the nematic behavior;[49,50] the anisotropy of the attractive van der Waals forces appears to be too small to account for the ordering.[48] Thus, the dominant roles are provided by the shape and packing of the molecules, under the influences of attractive forces which cause a reduction in the average intermolecular separation, but have little tendency to induce molecular alignment. In contrast to the earlier Maier–Saupe point of view,[46] the dispersive interactions contribute to the nematic to isotropic phase transition energy primarily through the total attractive force, whereas the anisotropy appears to be of secondary importance.

For the case of lipid bilayers, the acyl chains are effectively tethered to the aqueous interface by interactions of the polar head groups with water and with each other, together with the hydrophobic effect; their properties are more akin to those of smectic liquid crystals or to interfacial states of matter[40] than to bulk, isotropic liquids. The interactions of the polar head groups with each other and with the surrounding water molecules primarily influence the mean area per lipid molecule, and modulate indirectly the interactions between the chains. The roles of both short- and

(42) Meraldi, J.-P.; Schlitter, J. *Biochim. Biophys. Acta* **1981**, *645*, 183–192.
(43) Meraldi, J.-P.; Schlitter, J. *Biochim. Biophys. Acta* **1981**, *645*, 193–210.
(44) Longuet-Higgins, H. C.; Widom, B. *Mol. Phys.* **1964**, *8*, 549–556.
(45) Chandler, D. C.; Weeks, J. D.; Anderson, H. C. *Science* **1983**, *220*, 787–794.
(46) Maier, W.; Saupe, A. *Z. Naturforsch., Teil* A **1960**, *15*, 287–292.
(47) Marčelja, S. *J. Chem. Phys.* **1974**, *60*, 3599–3604.
(48) Wulf, A. *J. Chem. Phys.* **1976**, *64*, 104–109.
(49) Cotter, M. A. *J. Chem. Phys.* **1977**, *66*, 1098–1106.
(50) Gelbart, W. M.; Baron, B. A. *J. Chem. Phys.* **1977**, *66*, 207–213.

long-ranged interactions[17,39-43,51] have been discussed with regards to the main order–disorder transition to the liquid-crystalline state, as well as to the profiles of the orientational ordering of the acyl chain segments determined from ^{2}H NMR,[32] and their positional ordering determined from neutron diffraction studies.[52,53] The earlier theory of Maier and Saupe[46] for rod-like molecules in nematic fluids was extended to the individual chain segments of flexible lipid molecules by Marčelja;[41] in this picture the anisotropy of the attractive van der Waals interactions plays a dominant role in relating the microscopic order profiles of the chain segments to macroscopic thermodynamic properties. As mentioned above, this point of view has undergone some evolution. The energy of a particular chain conformation j is assumed to be the sum of a contribution from the internal configurational energy as given by the rotational isomeric model,[54] a dispersive contribution from attractive van der Waals forces, and a contribution from steric and other repulsive interactions which depends linearly on the chain configurational area $A(j)$. For the case of a lipid monolayer spread at the air–water interface, the steric repulsions correspond to a lateral pressure acting upon the lipid molecules, which is equal and opposite in direction to the applied external pressure. For a lipid bilayer, however, equilibrium thermodynamics requires that there is no net lateral pressure; i.e., $\gamma \equiv (\partial G_s/\partial A)_{T,P} = 0$, where dG_s is the change in the total surface Gibbs free energy due to a change in area dA at constant temperature T and bulk pressure P. The thermodynamic lateral pressure or surface tension γ is thus different from that of the free energy term linear in the area per chain as employed in the Marčelja theory and its descendents. Since the latter has the dimensions of surface tension, it is commonly referred to as a lateral chain pressure, but it is important to recognize that it is unrelated to any pressure which can be measured experimentally.

As discussed above, a weakness of the Marčelja theory for lipid bilayers,[41] and the earlier Maier–Saupe theory for nematic liquid crystals,[46] is that they overestimate the importance of the anisotropy of the attractive van der Waals interactions between the molecules.[42,43,48-50] Hard-sphere exclusions impose constraints on the molecular configurations[39,51] and are believed to be dominant in governing the averaged structures of lipid bilayers;[40,42,43] the van der Waals forces between aliphatic hydrocarbon chains are only weakly anisotropic.[55] While the balance of opposing attractive and repulsive intermolecular forces holds the density of the bilayer to within relatively narrow limits,[56] the surface density or mean area per chain, in the liquid-crystalline phase, can vary substantially with changes in thermodynamic variables such as temperature or concentration. Such a point of view is firmly grounded in our current understanding of the liquid[44,45] and liquid-crystalline[48-50] states of matter, as discussed above. Given that the averaged structure is determined primarily by short-ranged intermolecular repulsive forces, and that because of their amphiphilic character the lipid molecules are anchored by their polar ends to the aqueous interface, Dill and Flory[40] have solved a simple lattice model for the distribution of polymethylene acyl chain segments in the hydrocarbon interior of a lipid bilayer. The presence of gauche isomers leads to a shortening of the lengths of the individual chains projected along the bilayer normal, in the liquid-crystalline (L_α) phase, resulting in a broad distribution of the chain ends as a function of depth in the bilayer hydrocarbon region. The chain terminations then allow for increased configurational freedom of those segments near the center of the bilayer, thereby maintaining the density fixed at values typical of paraffinic fluids[40,56] and accounting for the characteristic plateau of the order profile.

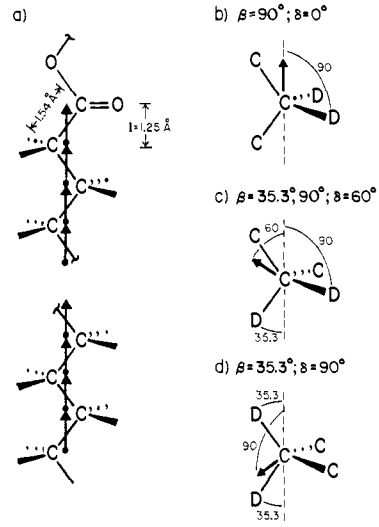

Figure 4. Simple diamond-lattice model for configurational statistics of polymethylene acyl chains in lipid bilayers (see text). The all-trans reference state of a polymethylene chain is indicated in (a), with virtual bonds of length l = 1.25 Å corresponding to projection of carbon–carbon bonds onto the long chain axis. Virtual bond vectors are represented by arrows normal to the planes defined by the two C–^{2}H bonds of the individual methylene groups; the contribution of the terminal segment is obtained by doubling the length of the penultimate virtual bond. The discrete segment orientations obtained by permuting two carbon (C) and two deuterium (D) atoms with respect to a central carbon atom on a diamond lattice are indicated in b–d. For clarity, virtual bond vectors are translated to the central carbon atom; the long chain axis is denoted by the vertical dashed lines. The angles between the individual C–^{2}H bond directions of the ith segment and the long axis are indicated by β_i, and the angles between the virtual bond vectors and the long axis by δ_i. The average chain length projected onto the long axis of the all-trans reference state is given by $\langle L \rangle = l\Sigma(\cos \delta_i)$. Note that the values of δ_i are not distinguished from their supplements, and thus chain configurations which fold back toward the initial segment are implicitly neglected. Inclusion of chain reversals leads to two additional segment orientations, which are identical with b and c except that the directions of the virtual bond vectors are reversed.

The model of Meraldi and Schlitter,[42,43] on the other hand, falls into the second category of a semiempirical or semiphenomenological theory.[38] Here the specific objectives are to provide greater insight into the ^{2}H NMR order profiles than would otherwise be possible, at perhaps some sacrifice in rigor,[42,43] and to extend the experimental data regarding the orientational fluctuations of the acyl chain segments to other quantities such as the spatial configurations of the chains. Meralidi and Schlitter[42,43] have applied the generalized van der Waals theory for nematic liquid crystals[49,50] to the flexible molecules of lipid bilayers; in this picture, the orientational ordering of the acyl chain segments is largely governed by the anisotropy of the short-ranged repulsive forces, as well as the overall strength of the intermolecular cohesion as discussed above. The steric or repulsive force acting over short distances (excluded volume effect) is accounted for by a term in the surface free energy linear in the area per chain, as in the Marčelja theory.[41] The anisotropy of the longer-ranged attractive forces is described by a spatially uniform, one-particle mean field, but in contrast to the Marčelja theory[41] plays a secondary role.[42,43] At present, the model of Meraldi and Schlitter appears quite successful in interpreting the ^{2}H NMR and neutron scattering data for phospholipid bilayers in terms of the orientational and positional fluctuations of their acyl chain segments, and in relating these quantities to other thermodynamic properties.

Qualitative Interpretation of ^{2}H NMR Order Profiles. With the above discussion in mind, we shall now return to a more detailed analysis of the experimental ^{2}H NMR data. Our treatment will emphasize the important qualitative aspects, in light of the conclusions and insights arrived at from both theoretical and experimental studies of the acyl chain configurational statistics of lipid bilayers. For the case of the di(per-^{2}H-16:0)PC bilayer in the L_α phase, the order profile obtained from the de-Paked ^{2}H

(51) Scott, H. L., Jr. *Biochim. Biophys. Acta* **1977**, *469*, 264–271.
(52) Büldt, G.; Gally, H. U.; Seelig, A.; Seelig, J.; Zaccai, G. *Nature (London)* **1978**, *271*, 182–184.
(53) Zaccai, G.; Büldt, G.; Seelig, A.; Seelig, J. *J. Mol. Biol.* **1979**, *134*, 693–706.
(54) Flory, P. J. *Statistical Mechanics of Chain Molecules*; Wiley-Interscience: New York, 1969.
(55) Salem, L. *J. Chem. Phys.* **1962**, *37*, 2100–2113.
(56) Nagle, J. F.; Wilkinson, D. A. *Biophys. J.* **1978**, *23*, 159–175.

NMR spectra (Figure 2) is in relatively good agreement with earlier studies of di(16:0)PC with specifically deuterated acyl chains.[32,35] The shape of the profile (with a well-defined plateau up to about the middle of the chain and a decrease in order in the central bilayer region) does not correspond to the behavior predicted by models which assume independent bond rotations.[54,58,59] Instead, the order profile must reflect steric constraints due to packing of the phospholipid molecules in the interior bilayer hydrocarbon region.[32]

The interpretation of the order profile of the di(16:0)PC bilayer has been previously discussed in some detail.[17,32,40,42,43] In what follows, it will be assumed that the phospholipid acyl chains are effectively tethered to the aqueous interface via the glycerol backbone and polar head groups, such that only those C–^{2}H bond orientations falling on a diamond- or tetrahedral-lattice are considered (Figure 4). The all-trans reference state of a saturated acyl chain is depicted in Figure 4a, and the three possible orientations of the polymethylene chain segments obtained by application of the rotational isomeric model[54] are given in Figures 4b–d. The various segment orientations are characterized by virtual bond vectors normal to the planes of the individual C^2H_2 groups,[32] where the angle between the normal to the plane spanned by the C–^{2}H bonds of the ith C^2H_2 group and the long chain axis is indicated by δ_i. It should be noted that the virtual bond vectors can point in either direction; that is, segment orientations corresponding to chain configurations which project deeper into the bilayer are not differentiated from those which fold back toward the bilayer surface.[42,43,60] The various segment orientations are assumed to interconvert at rates $>10^6$ s^{-1}, and rotational diffusion of the chains about the average bilayer normal could lead to the observed axially symmetric ^{2}H NMR spectra. It should also be noted that the various segment orientations in Figure 4 do not correspond directly to trans (t) and gauche (g) rotameric states. Thus, a total of six orientations are possible for each segment, i.e., trans or gauche with δ_i = 0, 60, or 90°, where the pentane rule[54] is assumed in which $g^{\pm}g^{\mp}$ sequences are sterically forbidden. If a single lipid monolayer is considered for calculational purposes, then one can distinguish two additional segment orientations which correspond to chain reversals; these are identical with Figure 4, parts b and c, except that the directions of the virtual bond vectors are reversed so that δ_i = 180 and 120°, respectively.[43] In this case a total of ten segment orientations are considered, i.e., trans or gauche with δ_i = 0, 60, 90, 120, and 180°.

Application of the statistical mechanical models of Marčelja[17,41] or Meraldi and Schlitter[42,43] to the ^{2}H NMR order profiles obtained for di(16:0)PC in the L_α phase[32] both predict that the predominant structural elements are trans segments aligned parallel to the average bilayer normal, i.e., (t, 0°); segments aligned perpendicular to this orientation, i.e., (t, 90°) and (g, 90°), are relatively improbable. Thus, an average parallel packing of the chains exists and is energetically the most favorable situation.[32] While similar results are obtained using the Marčelja theory[17] and the theory of Meraldi and Schlitter,[43] however, it should be noted that the physical bases of the two models are somewhat different as discussed earlier. Both of the above models predict that the probabilities of the various segment orientations are approximately constant as a function of position up to about the middle of the chain, thereby accounting for the plateau in the order profile (cf. Figure 2). The increased disorder in the bilayer central region is associated with a decrease in the probabilities of trans segments aligned parallel to the average bilayer normal,[17,43] so that the free volume which would otherwise exist due to chain terminations[40,57] is occupied. Thus, the acyl chains are packed at essentially liquid hydrocarbon density throughout the bilayer.[56] It does not appear as if any single type of conformation, such as kink or jog defects,[32,61] can account predominantly for the experimental order profiles of the di(16:0)PC bilayer at the segmental level.[2,17,43]

Qualitatively, then, it would appear that the shape of the order profile of the polyunsaturated (per-^{2}H-16:0)(22:6)PC bilayer, in the L_α phase, reflects an increase in the configurational freedom of the palmitoyl (16:0) chains relative to the di(16:0)PC bilayer at the same absolute temperature. It is unlikely that one can account for the ^{2}H NMR spectral differences in terms of differing contributions from relatively slow bilayer fluctuations (vide infra), as evinced by spin–lattice relaxation (R_{1Z}) studies (not shown). By analogy to the above results, the increased configurational freedom of the palmitoyl chains of the (per-^{2}H-16:0)(22:6)PC bilayer must reflect a loss or decrease of trans elements aligned parallel to the bilayer normal, i.e., (t, 0°), and a corresponding increase in the probabilities of the other segment orientations (cf. Figure 6 of ref 43). It follows that the interactions of the palmitoyl (16:0) chains with each other and with the docosahexaenoyl (22:6) chains in the hydrocarbon region of the polyunsaturated bilayer must differ significantly from those between the palmitoyl chains of the di(16:0)PC bilayer. Moreover, this effect is not simply a result of the lower transition temperature of the (16:0)(22:6)PC bilayer to the disordered liquid-crystalline phase ($\lesssim$−10 °C),[62] relative to that of the di(16:0)PC bilayer (41 °C). The above conclusions are supported on both experimental and theoretical grounds. Experimentally, Mely et al.[63] have shown rather clearly how the ^{2}H NMR order profiles depend on the mean cross-sectional area per chain ⟨A⟩, as determined from X-ray studies, for the case of lyotropic mesophases of potassium laurate soaps in the liquid-crystalline (L_α) state. Under conditions of temperature and water content for which the area per chain of the potassium laurate bilayer is comparable to that of phospholipid bilayers with two saturated chains in the L_α phase (30.7 Å^2), a similar order profile with a well-defined plateau is obtained. An increase in the area per chain at higher water contents and at higher temperatures leads to a decrease in the C–^{2}H bond segmental order parameters at all positions, and a decrease in the length of the plateau (Figure 5 of ref 63); the profile begins to approach that expected for a free chain tethered at one end to the aqueous interface.[58,59] Similar conclusions have been reached from ^{2}H NMR studies of potassium palmitate in the L_α phase.[25] These studies point clearly and in a direct experimental fashion to the importance of the area per chain, which is related to the surface free energy of the bilayer, in modulating the intermolecular chain configurational energies in the liquid-crystalline phase. The above picture is also consistent with theoretical statistical mechanical studies.[39,40,42,43,57] Dill and Flory[40] and Meraldi and Schlitter[43] have both called attention to the importance of the length of the plateau of the order profiles in interpreting the ^{2}H NMR data obtained for the bilayer hydrocarbon region. Their calculations indicate that the shape of the order profile and in particular the length of the plateau are highly dependent on the mean area per chain, which is related to the force–area isotherm of the corresponding lipid monolayer spread at the air–water interface.

Figures 1 and 2 show rather clearly that significant differences are observed in the order profiles of the palmitoyl (16:0) chains of the polyunsaturated and saturated bilayer systems. Qualitatively, it appears that the ^{2}H NMR spectra and derived order profiles of the (per-^{2}H-16:0)(22:6)PC and di(per-^{2}H-16:0)PC bilayers constitute useful probes of the configurational freedom of their acyl chains. The increased mobility of the palmitoyl chains of the (per-^{2}H-16:0)(22:6)PC bilayer, relative to the di(per-^{2}H-16:0)PC bilayer, can be accounted for in terms of an increase in the mean area per chain at which attractive and repulsive forces are balanced. Reference to the experimentally determined force–area isotherms for monolayers of saturated[64] and polyunsaturated[65] phospholipids shows that, in the liquid-crystalline state

(57) Gruen, D. W. R. *Biochim. Biophys. Acta* **1980**, *595*, 161–183.
(58) Seelig, J. *J. Am. Chem. Soc.* **1970**, *92*, 3881–3887.
(59) Hubbell, W. L.; McConnell, H. M. *J. Am. Chem. Soc.* **1971**, *93*, 314–326.
(60) Xu, Z.-C.; Cafiso, D. S. *Biophys. J.* **1986**, *49*, 779–783.
(61) Träuble, H. *J. Membr. Biol.* **1971**, *4*, 193–208.
(62) Sklar, L. A.; Miljanich, G. P.; Dratz, E. A. *Biochemistry* **1979**, *18*, 1707–1716.
(63) Mely, B.; Charvolin, J.; Keller, P. *Chem. Phys. Lipids* **1975**, *15*, 161–173.
(64) (a) Phillips, M. C.; Chapman, D. *Biochim. Biophys. Acta* **1968**, *163*, 301–313. (b) Vilallonga, F. *Ibid.* **1968**, *163*, 290–300.

at constant applied external pressure, the introduction of double bonds into the chains results in a progressive increase in the mean area per molecule relative to fully saturated phosphatidylcholines of the same chain lengths. The increased molecular area at constant lateral pressure is due to weaker van der Waals or cohesive interactions of the unsaturated chains relative to saturated chains.[55] At constant area per phospholipid, on the other hand, an increase in the lateral pressure is found with increasing polyunsaturation relative to saturated phosphatidylcholines with the same chain lengths. The increased lateral pressure at constant area per molecule appears to reflect steric repulsions due to the presence of one or more double bonds in the chains. Since it is the cross-sectional area of the individual chain configurations that is related to the steric or repulsive contribution to the configurational energy,[42,43] it follows from the ^{2}H NMR order profile of the (per-^{2}H-16:0)(22:6)PC bilayer that a decrease in the surface free energy term linear in the area per chain would be predicted by the Meraldi and Schlitter theory (Figure 4 of ref 43), corresponding to an increased mean area per chain as predicted by the Dill and Flory theory (Figure 3 of ref 40). It is possible that the area per molecule for the (16:0)(22:6)PC bilayer may be significantly greater than that for the di(16:0)PC bilayer; detailed X-ray and neutron scattering studies would appear to be desirable. Since the force–area isotherms of the corresponding lipid monolayers at the air–water interface are relatively steep for values of the area per molecule typical of phospholipid bilayers, rather appreciable changes in surface free energy could accompany relatively small differences in the molecular area. However, the correspondence betwen the states of lipid monolayers and bilayers is somewhat uncertain at present.[38]

Influences of Slow Motions. At this point it should be remarked that the above statistical mechanical analyses assume that contributions from relatively slow, collective bilayer motions, such as order–director fluctuations (ODF),[4,20,66-70] can be ignored to a first approximation.[1,17,32,42,43] In this regard, the reader should note that ODF or other slow motions would be expected to reduce all quadrupolar splittings proportionately,[32,66,70,71] and most likely cannot explain the qualitative differences in the shapes of the ^{2}H NMR spectra (Figure 1), or the different $|S_{CD}(i)|$ profiles (Figure 2) of the two bilayers. However, the quantitative interpretation of the ^{2}H NMR results and order profiles could be affected. While the segmental spin–lattice relaxation rates $R_{1Z}(i)$ of lipid bilayers in the MHz regime appear to include significant contributions from slow motions such as ODF,[4,20,66-69] their angular amplitude need not be great relative to faster trans-gauche isomerizations to provide a substantial relaxation contribution.[66,68,70] Thus, a self-consistent explanation of the ^{2}H NMR data is possible, in which the quadrupolar splittings in the L_α phase are chiefly influenced by segmental reorientations due to rotational isomerizations,[1,17,32,42,43,71-73] whereas the spin–lattice relaxation in the MHz regime and below could include significant contributions from slower motions such as ODF.[4,20,66-69]

Mean Projected Acyl Chain Length and Bilayer Thickness. The de-Paked ^{2}H NMR spectra and derived $|S_{CD}(i)|$ values can also be interpreted using a relatively simple statistical model[17,74] to yield an immediate estimate of the average or effective length of the acyl chains projected along the bilayer normal, to a first approximation. An estimate of the mean bilayer thickness is obtained as well[2,17,32] if one neglects interdigitation or displacement of the chains relative to each other in the two apposed monolayers. In what follows, the angular fluctuations of the deuterated segments of the palmitoyl (16:0) chains will be related to their positional fluctuations. Since the mean end-to-end chain length $\langle L \rangle$ is related to the average cross-sectional chain area $\langle A \rangle$ by $\langle L \rangle = V/\langle A \rangle$, where V is the molecular volume of the chain, such an approach is akin to the more detailed statistical mechanical models discussed above. For the case of ^{2}H NMR, one is looking *directly* at the properties of the individual chain segments, and thus computation of the energies of the various configurations is not required to calculate statistical properties such as mean end-to-end distances; the rotational isomeric state approximation[54] is adopted.[2,17,32]

The effective chain length $\langle L \rangle$ projected along the bilayer normal[17,32] can then be estimated in terms of the previously mentioned virtual bonds which connect the adjacent segments (Figure 4). The projected length of an individual chain segment in the all-trans reference state (cf. Figure 4a) is given by $l = 1.25$ Å. For the case of the terminal C^2H_3 group, a virtual bond cannot be defined in the same manner as for the chain C^2H_2 groups, owing to the C_{3v} symmetry. Since the orientation of the C_3 axis is governed by the rotational isomeric state of the preceding segment, however, one can simply choose the last virtual bond to be parallel to that of the final C^2H_2 chain segment, i.e., perpendicular to the C^2H_2 plane, which amounts to doubling the length of the penultimate virtual bond (vide infra). Upon averaging over all configurations (b–d of Figure 4), the contribution of each of the individual segments to the mean end-to-end distance of the acyl chains is given by $l\langle \cos \delta_i \rangle$; for simplicity, configurations which fold back toward the initial segment[42,43,60] are ignored. Then, the observed $|S_{CD}(i)|$ profiles can be used to estimate the mean chain length $\langle L \rangle$ relative to the all-trans reference state, as indicated below:[75]

$$\langle L \rangle = l\left[\left(\frac{n-m+1}{2}\right) - \sum_{i=m}^{n-1} S_{CD}(i) - 3S_{CD}(n)\right] \quad (3)$$

Based on geometrical considerations, the values of the segmental order parameters $S_{CD}(i)$ are presumed to be negative.[1] In eq 3, the number of carbon atoms in the fatty acyl chain is denoted by

(65) (a) Demel, R. A.; Geurts Van Kessel, W. S. M.; Van Deenen, L. L. M. *Biochim. Biophys. Acta* **1972**, *266*, 26–40. (b) Evans, R. W.; Tinoco, J. *Chem. Phys. Lipids* **1978**, *22*, 207–220.

(66) Brown, M. F. *J. Chem. Phys.* **1982**, *77*, 1576–1599.

(67) Brown, M. F.; Ribeiro, A. A.; Williams, G. D. *Proc. Natl. Acad. Sci. U.S.A.* **1983**, *80*, 4325–4329.

(68) Brown, M. F. *J. Chem. Phys.* **1984**, *80*, 2808–2831.

(69) Brown, M. F. *J. Chem. Phys.* **1984**, *80*, 2832–2836.

(70) Pace, R. J.; Chan, S. I. *J. Chem. Phys.* **1982**, *76*, 4228–4240.

(71) Seelig, J.; Niederberger, W. *Biochemistry* **1974**, *13*, 1585–1588.

(72) Stockton, G. W.; Polnaszek, C. F.; Tulloch, A. P.; Hasan, F.; Smith, I. C. P. *Biochemistry* **1976**, *15*, 954–966.

(73) (a) Pace, R. J.; Chan, S. I. *J. Chem. Phys.* **1982**, *76*, 4217–4227. (b) Grüen, D. W. R. *J. Phys. Chem.* **1985**, *89*, 146–153.

(74) It should be noted that the models of Seelig and Seelig (ref 32) and Schindler and Seelig (ref 17) are not identical. The former assumes that the motions of the acyl chain segments are axially symmetric about *both* the director *and* an axis normal to the plane of the two C–^{2}H vectors of a C^2H_2 group; i.e., a chain of segments is considered, each of which behaves analogously to a rod-like molecule in a nematic fluid. For such an axially symmetric diffusion model, in which motions perpendicular to the diffusion-tensor principal symmetry axis are restricted in their angular range, the observed C–^{2}H bond segmental order parameters, $S_{CD}(i)$, can be transformed to yield the order parameter of the normal to the plane of a C^2H_2 group, $S_{mol}(i)$, according to $S_{mol}(i) = -2S_{CD}(i)$. The order parameter of the local chain axis $S_{mol}(i)$ can then be compared to the experimental order parameters derived from nitroxide spin-label EPR studies of lipid bilayers (ref 1). Such an axially symmetric diffusion model has also been considered in an analysis of the spin–lattice relaxation rates $R_{1Z}(i)$ of lipid bilayers in the liquid-crystalline phase (ref 66–69). The model of Schindler and Seelig (ref 17), on the other hand, is a jump model for rotational isomerization, in which discrete segment orientations are considered; only axially symmetric motion about the director is assumed.

(75) Note that for typical values of $|S_{CD}(i)| < 0.2$, the second and third terms of eq 3 are less than the first term, and thus the largest influence on the calculated value of $\langle L \rangle$ is provided by the number of segments in the chain. Small but finite contributions to the observed values of $|S_{CD}(i)|$ may arise from chain configurations which fold back toward the bilayer surface (ref 43 and 60). While the latter can influence the shape of the order profiles substantially, and lead to a shortening of the plateau, their neglect in calculating $\langle L \rangle$ is not expected to introduce serious error. Any contributions from ODF to the observed order parameters would likewise not be expected to greatly alter the calculated result for $\langle L \rangle$. For example, assuming that slow motions lead to a reduction of the segmental order parameters (ref 32 and 68–71) by a multiplicative factor S of ~0.7–0.8, the estimated value of the mean effective chain length $\langle L \rangle$ would be increased by only ~1 Å, which is less than the uncertainty of X-ray and neutron diffraction data for phospholipid bilayers in the L_α phase. Use of eq 3 is then warranted as a first approximation.

n and the various segments are numbered beginning with the ester group. Contributions to the effective chain length from segments m through n are included, so that $\langle L \rangle$ is taken as extending from carbon atom C_{m-1} to the terminal carbon atom C_n; the last C–^{2}H bond of the chain is ignored. Because of the C_{3v} symmetry of the terminal C^2H_3 group, its residual quadrupolar coupling is projected along the last carbon–carbon bond, so that an additional coordinate transformation is necessary to resolve the contribution parallel to the long axis of the all-trans state.[72] The contribution to $\langle L \rangle$ from the terminal C^2H_3 segment is thus the same as that of the $(n-1)$th C^2H_2 segment; both are governed by the rotameric state probabilities of the $(n-1)$th carbon atom, and their order parameters are related by $S_{CD}(n-1) = 3S_{CD}(n)$, in good agreement with the experimental data in Figure 2. For the case of an all-trans chain, $S_{CD}(i \neq n) = -1/2$ and $S_{CD}(n) = -1/6$, which for $m = 2$ leads to $\langle L \rangle = (n-1)l$. Thus, eq 3 has the proper limiting behavior.

How is the effective or average length of the acyl chains related to the thickness of the bilayer hydrocarbon region? For the case of phospholipids in the L_α phase, some ambiguity exists in defining the average bilayer hydrocarbon thickness, since the ^{2}H NMR results depend on the orientational ordering of the fatty acyl chain segments, rather than their positional or spatial ordering as is the case for X-ray or neutron diffraction studies (vide supra). In the crystalline state,[76] the conformation of the diacylglycerol moiety of phosphatidylcholines and phosphatidylethanolamines is such that the two all-trans acyl chains are staggered or offset relative to each other by three methylene units or 3.7 Å. Thus, the initial segments of the two acyl chains have different spatial positions relative to the bilayer surface; the C_2 carbon atom of the *sn*-1 chain is lined up with the C_6 carbon of the *sn*-2 chain, whereas the C_2 carbon of the *sn*-2 chain is approximately lined up with the glycerol *sn*-2 carbon atom.[76] In the liquid-crystalline phase, it is believed that the phospholipid molecules are flexible[1-5,77] and undergo rapid fluctuations[4,35,66-69,78] involving preferred conformations[1,79] similar to those found in the crystalline state.[76] Rotational isomerization of the fatty acyl chains of phospholipids in the L_α phase will reduce their lengths projected along the bilayer normal,[17,32] as discussed previously, but not their relative displacement if the diacylglycerol moiety adopts an average conformation similar to that found in phospholipid crystals.[1,76,79] The average bilayer hydrocarbon thickness will then depend on the mean projected lengths of the two fatty acyl chains, as well as the extent of interpenetration of the chains of the two apposed monolayers. Here we shall define the effective or average length of the phospholipid chains as extending along an axis normal to the bilayer plane, from the C_1 carbon atom to the terminal carbon atom C_n for the case of the *sn*-1 chain, and from the C_2 carbon atom to the C_n atom for the *sn*-2 chain. If it is assumed that the all-trans reference state is aligned parallel to the average bilayer normal, and that chain interdigitation can be neglected, then the mean thickness of the bilayer hydrocarbon region is given in terms of the above model by $2\langle L \rangle$. For the case of di(16:0)PC with specifically deuterated acyl chains in the L_α phase, the bilayer hydrocarbon thickness estimated in this manner is in good agreement with the results of X-ray and neutron diffraction studies.[52,53,80]

The above simple model can then be used as an approximate framework or paradigm for interpreting the different ^{2}H NMR spectra and order profiles of the per-^{2}H-16:0 chains of the two bilayers. How do the effective lengths of the palmitoyl chains compare in the two cases? Is the hydrocarbon thickness of the polyunsaturated, (per-^{2}H-16:0)(22:6)PC bilayer similar to or significantly different from that of the saturated, di(per-^{2}H-16:0)PC bilayer? For the case of the di(per-^{2}H-16:0)PC bilayer in the L_α phase, due to inequivalence of the two acyl chains, different $|S_{CD}(i)|$ values are observed for their initial (C_2) methylene segments as well as those C^2H_2 groups toward the methyl termini (cf. Figure 2). The *sn*-2 chain is believed to have an initial segment orientation different from that of the *sn*-1 chain, and to start out parallel to the bilayer surface, before bending sharply at the C_2 carbon to allow for parallel packing of the chains in the bilayer hydrocarbon interior.[1,33,34] As a consequence, the $|S_{CD}(i)|$ values of the *sn*-2 chain segments of the di(per-^{2}H-16:0)PC bilayer appear slightly greater than those of the *sn*-1 chain (cf. Figure 2), corresponding to a slightly greater effective chain length. Neglecting the contribution of the C_2 segment for the case of the *sn*-2 chain (vide supra), the mean effective length of the *sn*-1 and *sn*-2 chains of the di(per-^{2}H-16:0)PC bilayer are calculated using eq 3 to be 12.3 and 11.5 Å, respectively, at 323 K. The small difference of 0.8 Å may reflect some limited interpenetration of the acyl chains in the L_α phase, which would tend to maintain the bilayer density near that of liquid hydrocarbons.[40,56] Assuming that chain interdigitation can be neglected, the thickness of the bilayer hydrocarbon region is calculated to lie in the range of 23.1 to 24.6 Å, in good agreement with the results of X-ray diffraction studies of di(16:0)PC in the L_α phase.[80] In the gel state ($L_{\beta'}$ phase), however, neutron diffraction studies[52,53] suggest that the two chains are out of step by approximately 1.5 carbon–carbon bonds, i.e., 1.8 Å; as mentioned previously, in the crystalline state an even larger difference of 3.7 Å is obtained.[76,79] Given the above values for $\langle L \rangle$ and using the molecular volume determined from dilatometry studies,[56] the mean cross-sectional areas of the palmitoyl chains at the *sn*-1 and *sn*-2 positions are calculated to be 35.4 and 35.5 Å^2, respectively. Assuming additivity of the individual chain areas, a mean cross-sectional area of 70.9 Å^2 is then obtained, which for a monolayer of di(16:0)PC at the air–water interface would correspond to a lateral pressure of $\pi \simeq 15$ mN m^{-1} at 318 K (45 °C).[64]

Although we have not studied the docosahexaenoyl (22:6) chain at the *sn*-2 position of the polyunsaturated, (per-^{2}H-16:0)(22:6)PC bilayer directly using ^{2}H NMR, as discussed above the palmitoyl (16:0) chain at the *sn*-1 position appears more configurationally disordered than is the case for the *sn*-1 palmitoyl chain of the di(per-^{2}H-16:0)PC bilayer. According to eq 3, the effective or mean projected length of the *sn*-1 palmitoyl chain of the (per-^{2}H-16:0)(22:6)PC bilayer is estimated to be 11.7 Å; an effective shortening of about 0.6 Å is found vs. the *sn*-1 chain of the di(per-^{2}H-16:0)PC bilayer, at the same absolute temperature of 323 K. The corresponding value obtained for the chain cross-sectional area (vide supra) is $\langle A \rangle = 37.2$ Å^2. Thus, rather small differences in the effective chain length $\langle L \rangle$ and mean area $\langle A \rangle$ could underlie the different ^{2}H NMR spectra (Figure 1) and derived order profiles (Figure 2) of the two bilayers. This is due partly to the fact that the *sn*-1 palmitoyl chains are substantially disordered in both cases, as well as to the sensitivity of the ^{2}H NMR spectra to rather small conformational differences.[81] The above observations could in turn imply that the effective length of the polyunsaturated, docosahexaenoyl (22:6) chain, at the *sn*-2 position of the (per-^{2}H-16:0)(22:6)PC bilayer, is similar to that of the *sn*-2 palmitoyl chain of the saturated, di(per-^{2}H-16:0)PC bilayer, in spite of the greater number of carbon atoms. This could be due to coiled or helical configurations of the 22:6 chain, as suggested by an inspection of molecular models, in which case the hydrocarbon thicknesses of the two bilayers could be rather similar. Alternatively, the polyunsaturated and saturated acyl chains of the two apposed monolayers of the (per-^{2}H-16:0)-(22:6)PC bilayer could be interdigitated in a way that leads to increased orientational disorder of the *sn*-1 palmitoyl chain vis-ã-vis that of the di(per-^{2}H-16:0)PC bilayer. In this case, significant differences in the hydrocarbon thicknesses of the polyunsaturated and saturated bilayers would be possible. At present, one cannot distinguish unequivocally between the above interpretations, and

(76) (a) Hitchcock, P. B.; Mason, R.; Thomas, K. M.; Shipley, G. G. *Proc. Natl. Acad. Sci. U.S.A.* **1974**, *71*, 3036–3040. (b) Pearson, R. H.; Pascher, I. *Nature (London)* **1979**, *281*, 499–501.
(77) Luzzatti, V.; Husson, F. *J. Cell Biol.* **1962**, *12*, 207–219.
(78) Brown, M. F. *J. Magn. Reson.* **1979**, *35*, 203–215.
(79) Hauser, H.; Pascher, I.; Pearson, R. H.; Sundell, S. *Biochim. Biophys. Acta* **1981**, *650*, 21–51.
(80) (a) Lis, L. J.; McAlister, M.; Fuller, N.; Rand, R. P.; Parsegian, V. A. *Biophys. J.* **1982**, *37*, 657–666. (b) Lewis, B. A.; Engelman, D. M. *J. Mol. Biol.* **1983**, *166*, 211–217.
(81) (a) Brown, M. F.; Seelig, J. *Nature (London)* **1977**, *269*, 721–723. (b) Brown, M. F.; Seelig, J. *Biochemistry* **1978**, *17*, 381–384.

further work is necessary. Moreover, the neglect of folded-back chain configurations could mean that larger differences in the effective length $\langle L \rangle$ could exist than predicted by eq 3, so that further interpretation may require a more elaborate statistical mechanical analysis.

Finally, the isobaric coefficient of thermal expansion $\alpha \equiv (\langle L \rangle^{-1} \partial \langle L \rangle / \partial T)_P$ can be estimated from the temperature dependence of the ^{2}H NMR quadrupolar splittings[32] of the per-^{2}H-16:0 chains of the two bilayers using eq 3. An average value of $\alpha \simeq -1.5 \times 10^{-3}$ K^{-1} is obtained in both cases, consistent with previous X-ray[77,82] and ^{2}H NMR studies[32,72] of various phospholipid bilayers in the L_α phase.

5. Conclusions and Biological Significance

To summarize, we have discovered significant differences in conformation-dependent properties of the acyl chains of polyunsaturated and saturated phospholipid bilayers using ^{2}H NMR. The results lend themselves to a simplified statistical mechanical interpretation, and may eventually contribute to a better understanding of the biological roles of polyunsaturated phospholipids in membranes. Qualitatively, the behavior of the saturated chains of bilayers composed of asymmetric, saturated–polyunsaturated phosphatidylcholines appears to reflect an increase in their configurational freedom relative to symmetric, disaturated phospholipids. Thus, the lateral chain packing in polyunsaturated phospholipid bilayers may be significantly different from that in bilayers composed of phospholipids with two saturated acyl chains. The increased chain configurational freedom can be explained in terms of an increase in the equilibrium area at which attractive and repulsive forces acting upon the chains are balanced. This in turn could have implications for the energetics of functionally linked, membrane protein conformational changes. For example, given that an intrinsic membrane protein increases its cross-sectional area $A^{(p)}$ in undergoing a conformational change, the relative free energies of the initial and final states could include a contribution from the work of expansion against the lateral chain pressure π_c, given by

$$W = \int \pi_c \mathrm{d}A^{(p)} \cong 2\pi_c \Delta A^{(p)} \quad (4)$$

where the factor of two accounts for the apposed monolayers of the lipid bilayer. The above may provide one means by which lipid–protein interactions are coupled to specific biological membrane functions; other contributions may also be important and further experimental and theoretical investigations are necessary.

Acknowledgment. Thanks are due to Ken Dill, Thomas McIntosh, Jean-Paul Meraldi, Joachim Seelig, and Wilma Olson for their helpful criticisms of the manuscript. We are also grateful to Jeffrey Ellena and William Shoup for valuable assistance and to Edward Sternin and Myer Bloom for a listing of their de-Pakeing program. This research was funded by Grant EY03754 from the U.S. National Institutes of Health, and by the Thomas F. Jeffress and Kate Miller Jeffress Memorial Trust. A.S. was supported by a National Science Foundation predoctoral fellowship and J.M.B. by National Institutes of Health Postdoctoral Fellowship EY05746. M.F.B. is the recipient of Research Career Development Award EY00255 from the National Eye Institute.

(82) Rand, R. P.; Pangborn, W. A. *Biochim. Biophys. Acta* **1973**, *318*, 299–305.

Multifrequency Electron Spin Resonance of Molybdenum(V) and Tungsten(V) Compounds

Graeme R. Hanson,*[1a,c] Graham L. Wilson,[1a] Trevor D. Bailey,[1a,d] John R. Pilbrow,*[1b] and Anthony G. Wedd*[1a]

Contribution from the Department of Chemistry, La Trobe University, Bundoora, Victoria 3083, Australia, and the Department of Physics, Monash University, Clayton, Victoria 3168, Australia.
Received August 12, 1986

Abstract: The ESR spectra of a selection of molybdenum(V) and tungsten(V) compounds have been examined as a function of microwave frequency. In particular, reduced line widths at lower (S band: 2–4 GHz) microwave frequencies allow detection of ^{14}N, ^{1}H, ^{17}O, ^{77}Se, and ^{35,37}Cl superhyperfine interactions in certain of the following complexes: $[Mo(abt)_3]^-$ ($abtH_2$ = *o*-aminobenzenethiol), $[MO(XPh)_4]^-$ (M = Mo, W; X = S, Se), and *cis*-$[MoO(qtl)_2X]$ (X = Cl, Br; qtlH = quinoline-8-thiol). The redistribution of spectral information as a function of frequency, together with computer simulation, has allowed the determination of the hyperfine matrix and its relative orientation to the **g** matrix, in most cases. A d_{z^2}-based ground state is assigned to $[Mo(abt)_3]^-$ in contrast to d_{xy}-based ground states for the oxo-molybdenum(V) complexes. Axially symmetric sites are present in $[MO(XPh)_4]^-$ and monoclinic (C_s) sites in *trans*-[MoOL(DMF)]$^+$ (L = salen, salophen). The results provide strong motivation for a wider examination of transition metal species at lower microwave frequencies.

Recent advances in technology,[2–6] and the development of the loop-gap resonator in particular, have permitted more convenient measurement of electron spin resonance as a function of frequency. The advantages of such measurements include the following.[7]

1. A Potential Gain in Resolution. Reduction of line width can occur as the frequency is lowered, resulting in the resolution of metal and ligand hyperfine structure, as has been seen in frozen glass spectra of several copper(II) complexes[8,9] and proteins.[10,11] This narrowing can be attributed to a reduction in *g* strain (or correlated *g*–*A* strain[9]), caused by the environment of the electron

(1) (a) La Trobe University. (b) Monash University. (c) Present address: Department of Physics, Monash University. (d) Present address: School of Chemistry, University of N.S.W., Kensington, N.S.W., Australia.
(2) Hyde, J. S.; Froncisz, W. *J. Magn. Reson.* **1982**, *47*, 515.
(3) Hyde, J. S.; Yin, J. J.; Froncisz, W.; Feix, J. B. *J. Magn. Reson.* **1985**, *63*, 142.
(4) Johansson, B.; Haraldson, S.; Pettersson, L.; Beckman, O. *Rev. Sci. Instr.* **1974**, *45*, 1445.
(5) Brown, G. *J. Phys. E* **1974**, *7*, 635.
(6) Dahlberg, E. D.; Dodds, S. A. *Rev. Sci. Instr.* **1981**, *52*, 472.
(7) Froncisz, W.; Hyde, J. S. *Annu. Rev. Biophys. Bioeng.* **1982**, *11*, 391.
(8) Abdrachmanov, R. S.; Ivanova, T. A. *J. Mol. Struct.* **1973**, *19*, 638; **1978**, *46*, 229.
(9) Froncisz, W.; Hyde, J. S. *J. Chem. Phys.* **1980**, *73*, 3123.
(10) Froncisz, W.; Scholes, C. P.; Hyde, J. S.; Wei, Y.-H.; King, T. E.; Shaw, R. W.; Beinert, H. *J. Biol. Chem.* **1979**, *254*, 7482.
(11) Froncisz, W.; Aisen, W. *Biochem. Biophys. Acta* **1982**, *700*, 55.

0002-7863/87/1509-2609$01.50/0